AD-A191 699

AFGL-TR-87-0276

INFLUENCE OF SCATTERING ON SEISMIC WAVES:
PHYSICAL MECHANISMS CONTRIBUTING TO ATTENUATION IN THE CRUST

M. Nafi Toksöz
Ru-Shan Wu
Denis P. Schmitt

Earth Resources Laboratory
Department of Earth, Atmospheric, and
 Planetary Sciences
Massachusetts Institute of Technology
Cambridge, Massachusetts 02139

30 September 1987

Scientific Report No. 2

APPROVED FOR PUBLIC RELEASE; DISTRIBUTION UNLIMITED

88 2 12 062

ADA191699

REPORT DOCUMENTATION PAGE

1a. REPORT SECURITY CLASSIFICATION	1b. RESTRICTIVE MARKINGS
Unclassified	

2a. SECURITY CLASSIFICATION AUTHORITY	3. DISTRIBUTION / AVAILABILITY OF REPORT
	Approved for public release; distribution unlimited
2b. DECLASSIFICATION / DOWNGRADING SCHEDULE	

4. PERFORMING ORGANIZATION REPORT NUMBER(S)	5. MONITORING ORGANIZATION REPORT NUMBER(S)
	AFGL-TR-87-0276

6a. NAME OF PERFORMING ORGANIZATION	6b. OFFICE SYMBOL (If applicable)	7a. NAME OF MONITORING ORGANIZATION
Earth Resources Laboratory, Dept. of Earth, Atmospheric, and Planetary Sciences		Air Force Geophysics Laboratory

6c. ADDRESS (City, State, and ZIP Code)	7b. ADDRESS (City, State, and ZIP Code)
Massachusetts Institute of Technology Cambridge, MA 02139	Hanscom AFB, MA 01731

8a. NAME OF FUNDING / SPONSORING ORGANIZATION	8b. OFFICE SYMBOL (If applicable)	9. PROCUREMENT INSTRUMENT IDENTIFICATION NUMBER
		F19628-86-K-0004

8c. ADDRESS (City, State, and ZIP Code)	10. SOURCE OF FUNDING NUMBERS			
	PROGRAM ELEMENT NO.	PROJECT NO.	TASK NO.	WORK UNIT ACCESSION NO.
	61101E	6A10	DA	BF

11. TITLE (Include Security Classification)
Influence of Scattering on Seismic Waves: Physical Mechanisms Contributing to Attenuation in the Crust (unclassified)

12. PERSONAL AUTHOR(S)
M. Nafi Toksöz, Ru-Shan Wu, Denis P. Schmitt

13a. TYPE OF REPORT	13b. TIME COVERED	14. DATE OF REPORT (Year, Month, Day)	15. PAGE COUNT
Scientific Rept. No.2	FROM 8/1/86 TO 1/31/87	1987 September 30	60

16. SUPPLEMENTARY NOTATION

17. COSATI CODES			18. SUBJECT TERMS (Continue on reverse if necessary and identify by block number)
FIELD	GROUP	SUB-GROUP	seismic attenuation, Q, crust, strong motion, Rg, coda, fluid flow, fractures, anelasticity

19. ABSTRACT (Continue on reverse if necessary and identify by block number)

The mechanisms contributing to the attenuation of earthquake ground motion in the distance range of 10 to 200 km are studied with the aid of laboratory data, coda waves and strong motion attenuation measurements in the northeastern United States and Canada and theoretical models. The relative contributions to attenuation of anelasticity of crustal rocks (constant Q), fluid flow and scattering are evaluated. Scattering is found to be strong with albedo of $B_0 = 0.9$ and scattering extinction length of about 17 km. The intrinsic attenuation in the crust can be explained by a high constant Q ($500 \leq Q_0 \leq 2000$) and a frequency dependent mechanism most likely due to fluid effects in rocks and cracks. A fluid-flow attenuation model gives a frequency dependence ($Q \simeq Q_0 f^{0.5}$) similar to those determined from the analysis of coda waves of regional seismograms.

20. DISTRIBUTION / AVAILABILITY OF ABSTRACT	21. ABSTRACT SECURITY CLASSIFICATION
☒ UNCLASSIFIED/UNLIMITED ☐ SAME AS RPT. ☐ DTIC USERS	unclassified

22a. NAME OF RESPONSIBLE INDIVIDUAL	22b. TELEPHONE (Include Area Code)	22c. OFFICE SYMBOL
James F. Lewkowicz	617/377-3028	LWH

DD FORM 1473, 84 MAR ____ 83 APR edition may be used until exhausted. ____ SECURITY CLASSIFICATION OF THIS PAGE

All other editions are obsolete.

Table of Contents

Accession For	
NTIS GRA&I	☑
DTIC TAB	☐
Unannounced	☐
Justification	
By	
Distribution/	
Availability Codes	
Dist	Avail and/or Special
A-1	

Preface

The following document is the text of a paper titled "Physical mechanisms contributing to seismic attenuation in the crust" by M. N. Toksöz, R. S. Wu and D. P. Schmitt. This paper has appeared in the Proceedings of the NATO ASI "Strong Ground Motion Seismology, M. O. Erdik and M. N. Toksöz, eds., pp. 225–247, published by Reidel in 1987. The work was supported by the U. S. Geological Survey and the Air Force Geophysics Laboratory under contract F19628-86-K-0004; the paper is being submitted as a Scientific Report for this contract.

Introduction

The amplitude of seismic waves from an earthquake source decreases with increasing distance because of geometric spreading and because of attenuation resulting from the absorption and conversion of seismic energy into heat. Just like seismic velocities, the attenuation properties vary in the crust both as a function of depth and laterally. Generally, attenuation variations are larger by about one order of magnitude than the velocity variations. In this paper, we study the physical processes contributing to seismic attenuation in the crust. The primary mechanisms we consider are the anelasticity of crustal rocks, scattering due to heterogeneities, and fluid movements within pores and cracks in the crust. These are shown schematically in Figure 1.

We consider attenuation in the distance range of 10 to 100 km. This interval is ideal for several important reasons. At distances shorter than about 10 km from the source, non-linear behavior of materials due to high strains ($\epsilon \geq 10^{-5}$) can dominate. At distances greater than 100 km, the geometric spreading effects, due to velocity-depth functions and multiple branches of travel-time curves, become site-specific and uncertain. Another important factor for favoring this distance range is that a considerable amount of new attenuation data has been obtained both from strong motion records and the analysis of seismic coda waves.

Before reviewing the attenuation data, it is important to define the terminology. The attenuation for a given wave type (P or S) is defined as the inverse of the quality factor Q, and related to other measures by:

$$\frac{1}{Q} = \frac{\alpha V}{\pi f} = \frac{\delta}{\pi} \tag{1}$$

where α is the attenuation coefficient, V the wave velocity, f the frequency, and δ the logarithmic

1

decrement.

Attenuation Q^{-1} or the quality factor Q are dimensionless quantities. Physically, Q^{-1} is equal to the ratio of energy dissipated per cycle to the total energy. For small attenuation, (i.e. $Q^{-1} \leq 0.1$), additional relationships can be established in terms of stress-strain relationships:

$$\frac{1}{Q} = \frac{M_I}{M_R} = \tan \phi \simeq \phi \tag{2}$$

where M_I and M_R are the imaginary and real parts of the appropriate elastic modulus ($M = M_R + iM_I$) and ϕ is the phase lag of the strain behind the stress (i.e., loss tangent). The dimension of the attenuation coefficient α is generally given as dB/unit length or nepers per unit length. The relationship between the two is α(dB/unit length) = 8.686 α(nepers/unit length).

Most of the data for crustal attenuation comes from coda waves (Aki and Chouet, 1975; Aki, 1980; Pulli, 1984; Singh and Herrmann, 1983; Singh, 1985; Gupta et al., 1983; Rautian and Khalturin, 1978; Roecker et al., 1982; Herrmann, 1980). These measurements generally give attenuation that decreases with frequency in the frequency range of f =0.5 to 25 Hz. Some typical coda Q values are:

$$Q_c(f) = 460 f^{0.4} \tag{3}$$

for New England (Pulli, 1984);

$$Q_c(f) = 1000 f^{0.2} \tag{4}$$

for the Central United States (Singh and Hermann, 1983); and

$$Q_c(f) = 150 f^{0.45} \tag{5}$$

for the Western United States (Singh and Hermann, 1983).

2

The increase of Q with frequency and the high values ($Q \geq 1000$) at frequencies above 10 Hz in the Eastern United States cannot be reconciled with the laboratory measurements of Q in crustal rocks (see Toksöz and Johnston, 1981 for a comprehensive compilation). Most laboratory data suggest that, at least for dry rocks, Q is independent of frequency (Birch and Bancroft, 1938; Peselnick and Outerbridge, 1961; Klima et al., 1964; Knopoff, 1964; Pandit and Savage, 1973; Toksöz et al., 1979; Nur and Winkler, 1980; Johnston and Toksöz, 1980; Tittman et al., 1981). Water saturation generally decreases Q values of both P and S waves, although the decrease is much greater for S-waves than for P-waves.

Q increases with increasing confining pressure. However, the laboratory Q values at pressures of 2 kilobars or more in crystalline rocks are generally less than 1000 (Klima et al., 1964; Bradley and Fort, 1966; Mason et al., 1970). It is only in the case of totally outgassed and volatile free rocks that Q values of 2000 or more have been obtained (Clark et al., 1980; Tittman et al., 1974).These values have been observed in the completely dry environment of the moon (Dainty et al., 1976). The Earth's crust is not free of water and volatiles and the high Q values cannot be attributed to dehydration. The high Q values still need to be explained.

Although Q is independent of frequency in dry rocks, it may be frequency dependent in saturated and partially saturated rocks (Gardner et al., 1964; Winkler and Nur, 1979; Spencer, 1981; Tittman et al., 1981). The saturation may produce relaxation peaks at certain frequencies and increase and decrease of Q on two sides of a peak. The question we wish to investigate is whether such relaxation phenomena and fluid motions can explain the frequency dependence of crustal Q values measured from coda waves.

3

Attenuation measurements in the Earth using coda waves or strong motion seismograms include the contribution of scattering due to heterogeneities, fluid-flow effects in fractures and intrinsic anelasticity of crustal rocks. The laboratory measurements incorporate effects of anelasticity and fluids in pores and coating the grains. In order to compare the Earth data with the laboratory results, it is necessary to separate the effects of scattering and fluid motions in fractures. In this study, we do this in two steps. First, we calculate the scattering effects. Then we interpret the remaining attenuation and its frequency dependence in terms of constant-Q type intrinsic attenuation and fluid flow attenuation. Each of these steps are model-dependent so that the results depend on the validity of the models.

Scattering Attenuation

Scattering of elastic waves propagating in a heterogeneous medium contributes to the attenuation of these waves. Scattering attenuation is not an energy dissipation mechanism, but only an energy redistribution in space and time, therefore, it is a geometric effect. Under the single scattering approximation, the scattering attenuation cannot be separated from the intrinsic attenuation. In order to separate these two attenuation mechanisms, we need to use the multiple scattering theory. There is no general solution for the multiple scattering theory. However, several special cases cases have been studied (O' Doherty and Anstey, 1971; Kopnichev, 1977; Dainty and Toksöz, 1977, 1981; Richards and Menke, 1983; and Gao et al., 1983a, b). Wu (1984, 1985) formulated the multiple scattering problem in the frequency domain using radiative transfer theory. In the case of isotropic scattering with a point source in an infinite random medium, an exact solution can be obtained (Appendix A).

Figure 2 shows the distribution of seismic wave energy with distance calculated by the theory. In the figure, the energy density is normalized by the extinction length L_e, which is the reciprocal of the extinction coefficient η_e:

$$L_e = 1/\eta_e$$
$$\eta_e = \eta_a + \eta_s$$

(6)

where η_a is the energy absorption coefficient due to anelasticity of the medium and η_s is the scattering coefficient which is defined as the total scattered power by a unit volume of random medium per unit incident power flux density. Note that η_a is related to the attenuation coefficient given in equation (1) by $\eta_a = 2\alpha$. In Figure 2 the curve shapes change depending on the seismic

albedo B_0 of the medium, which is defined as:

$$B_0 = \frac{\eta_s}{\eta_e} = \frac{\eta_s}{\eta_s + \eta_a} \qquad (7)$$

For the case of large albedo ($B_0 > 0.5$), i.e. when the medium is strongly heterogeneous, and scattering is significant, the curves are of arch shape. The maxima of the curves depend on the extinction coefficient ($\eta_e = \eta_s + \eta_a$). Therefore it is possible to obtain B_0 and η_e from the energy density-distance curves, and thus separate the scattering effect from the intrinsic attenuation.

The theory has been applied to local earthquakes in Hindu Kush region (Wu, 1984; Wu and Aki, 1985) with the conclusion that the scattering attenuation in that region is not the dominant factor ($B_0 \leq 0.5$). In this study, we look at the attenuation data in the eastern United States where anelastic attenuation may be low.

Figures 3a and 3b are the strong motion data (pseudo velocity) in Northeastern America for the case of $f = 5$ Hz and 1 Hz respectively (with 5% damping). The solid lines in the figures are the best fits to the data. If we assume that the received strong motions are composed of both the direct arrivals and the scattered waves, then we can compare curves given in Figure 2 with the data to obtain the seismic albedo B_0 and the intrinsic quality factor Q_a. In Figure 4, the PSV data are corrected for the geometric spreading ($1/R$ for body waves) and then squared to compare with the theoretical predictions. The best theoretical curves are also drawn in the figure. We can see that in the first 100 km the fit between theory and data is generally good except for a few points which are very close to the source. For greater distances, the data gradually deviate from the theory and become flatter. This may be due to the dominance of L_g waves at great distances. The discrepancy of data and theory at very close distances is probably due to the non-linear effects. From these

6

Table 1: Medium parameters at $f = 1$ and $f = 5$ Hz based on multiple scattering theory

Parameter	$f = 1$ Hz	$f = 5$ Hz
L_e	15 km	15 km
B_0	0.9	0.9
η_s	0.06/km	0.06/km
$L_s(= 1/\eta_s)$	16.7 km	16.7 km
η_a	0.0067 km	0.0067 km
$L_a(= 1/\eta_a)$	150 km	150 km
$Q_s(= kL_s)$	30	150
$Q_a(= kL_a)$	270	1350

comparisons of data with theory, we obtain the average seismic albedo $B_0 = 0.9$ and the extinction length $L_e = 15$ km for both the 1 Hz and 5 Hz waves. The medium parameters based on these values are listed in Table 1. In Figure 5 we plot the theoretical curves of PSV-distance relation for different seismic albedo B_0 when the extinction length is fixed at 15 km. A smaller albedo means a smaller intrinsic Q and therefore has a steep decrease of amplitude with distance. Figure 6 shows different curves of different albedos when the intrinsic Q is fixed at $Q_a = 1350$. We can see that the strong scattering will make the apparent attenuation much bigger than the intrinsic attenuation when the distance is larger than the absorption extinction length, L_a. However, the amplitude change is not exponential for small distances.

Results given in Table 1 give a good fit to the data with a consistent set of parameters at $f=1$ Hz and $f=5$ Hz. They suggest a frequency dependent anelastic Q with $Q_a=270$ at 1 Hz and $Q_a=1350$ at 5 Hz. As it was discussed in the first section while reviewing the laboratory data, such

7

variation of Q with frequency cannot be explained without a relaxation mechanism. In the crust, the fluids may provide such a mechanism.

Effects of Fluids on Attenuation

A fracture medium can be viewed as a fully saturated porous material of low porosity and relatively high permeability. Following Biot (1956a, b; 1962), such a finite porosity rock is modeled as a statistically isotropic material composed of a solid elastic matrix permeated by a network of interconnected pores saturated by a compressible viscous liquid. The liquid phase is then continuous and the wavelength of the signal is considered to be large compared to the characteristic pore dimension. As it allows the analysis of the propagation of a total wavefield, this model has been the basis of numerous studies is various fields. However, it was not until recently that Plona (1980) and Plona and Johnson (1980) experimentally demonstrated the validity of the theory. It predicts the existence of three types of body waves : a compressional wave of the first kind (P_1), which displays high velocity and quasi elastic properties; a compressional wave of the second kind (P_2), associated with low velocity and quasi viscous characteristics, and a shear wave. All three body waves are dispersive and dissipative : their velocities and attenuations are frequency dependent. In this study, we will focus on the traditional P (i.e, P_1) and S waves.

Energy dissipation due to fluid flow is related to the relative motion of the two phases which are coupled through inertial and viscous forces. These are characterized by a viscous $(b(\omega))$ and a mass $(\rho_{22}(\omega))$ coupling coefficients which can be expressed as functions of the imaginary and real parts (respectively) of the *spectral signature* of the material which is itself function of the pore shape and the pore geometry (Auriault et al., 1985); Schmitt, 1985). These forces are of the same order of

9

magnitude for a so-called critical frequency f_{ci} given by:

$$f_{ci} = \frac{b(o)}{2\pi \rho_{22}(0)} = \frac{\nu\phi}{2\pi \tilde{k}\rho_f \theta} \qquad (8)$$

where ν is the dynamic viscosity of the fluid, ρ_f is the fluid density, θ is a coefficient characteristic of the pore shape and pore geometry and $\tilde{k}$ is the intrinsic permeability of the porous material.

Below the critical frequency, i.e. in the *low* frequency range, the viscous forces are dominant and the fluid flow follows Poiseuille's law. The attenuation (Q^{-1}) of P and S waves is then proportional to frequency. In the *high* frequency range, i.e. above the critical frequency, the viscosity effect takes place in a very thin boundary layer close to the pore wall and the inertial forces become dominant. The attenuation of both P and S waves is then proportional to the inverse of the square root of the frequency. The attenuation is maximum at the critical frequency for both the P and the S waves. The theoretical prediction of the behavior of the attenuations above the critical frequency approximates quite well the observed frequency dependence (i.e., Q is proportional to $f^{0.4}$ in the Northeast and to $f^{0.45}$ in the West). It implies that the critical frequency is $f_{ci} \leq 1$ Hz.

In addition to the fluid flow attenuation, the P and S waves are attenuated due to Coulomb friction between grains of the rock. This attenuation is independent of frequency (Walsh, 1966). In a porous material, elastic constants can be expressed as functions of the bulk moduli of the constitutive grains K_s, the skeleton K_b and the fluid K_f, the shear modulus of the skeleton μ_b and the porosity ϕ (see Appendix B). The constant Q of the solid can be introduced through equation $B-4$.

To calculate attenuation due to fluid flow, we take a crustal crystalline rock model saturated with water. The physical parameters of the medium are given in Appendix B. The viscosity used

10

for the fluid is 0.2 centipoise. This value corresponds to water viscosity at a temperature of $100°C$.

The critical frequency defined by equation 8 is a function of the pore geometry, the permeability and the porosity. To obtain a critical frequency close to 1 Hz, using cylindrical ducts in two perpendicular directions, typical values of permeability and porosity are: 50 darcies, 0.5%; 100 darcies, 1%;and 200 darcies, 2%. These sets of parameters give a critical frequency of 1.21 Hz. If instead of ducts we use fractures of equivalent permeability, we obtain fracture apertures of 20 to 800 μm. With increasing porosity, this leads to fracture densities of 0.6, 1.2, and 2.5 per meter. Although the fracture widths and densities are not unrealistic for the shallow part of the crystalline crust where drillings core and borehole studies have been done, it is necessary to do more detailed modelling to evaluate the effects of interconnected fractures systems.

Figures 7a, b display the velocity dispersion and attenuation for P and S waves between 0.1 and 100 Hz due to fluid flow. For both waves, the velocity dispersion is small. The maxima of attenuation decreases with decreasing porosity because of smaller volume of fluid. The attenuation of the S wave is much greater than that of the P wave. For shear waves Q values at successive maxima are equal to 700, 1400, and 2800. At 5 Hz, we obtain shear Q values of 1100, 2000 and 4000, in the range of Q values given in Table 1.

Adding the attenuation in the solid as constant Q raises the total attenuation values. Figures 8a,b display the results obtained with addition of constant quality factors of 500. For the S wave, the attenuation maxima now obtained corresponds exactly to the sum of the inverse of both quality factors (this rule does not hold for the P waves because of the presence of the P_2 wave). For shear waves, the Q values at 1.2 Hz for the three models are 290, 370 and 420, respectively. These fall

11

in the range of Q values given in Table 1. For a higher Q, any $Q=2000$, shear Q values will more nearly approximate those given above. If we accept anelastic Q values given in Table 1 ($Q = 270$ at 1 Hz and $Q = 1350$ at 5 Hz), then we need to combine the fluid flow mechanism with a constant Q value of 500 to 2000 in order to explain the attenuation. The upper limit of 2000 is obtained from the minimum plausible solid attenuation (Clark et al., 1980).

These simple calculations show that a combination of attenuation due to solid friction (constant Q) and fluid flow can explain the attenuation values after removing the scattering effects. The importance of fluid flow contribution is that it can explain the frequency dependence of observed intrinsic Q values of S waves.

Discussion and Conclusions

In this paper, we proposed three mechanisms to explain the attenuation of earthquake ground motion in the distance range of 10 to 100 km. These include multiple scattering due to heterogeneities in the crust, Coulomb friction in rocks and viscous dissipation due to fluid motions in cracks. In order to determine the relative importance of these mechanisms, we considered the Q measurements made in the laboratory, determined by the decay of coda waves of local seismograms and the amplitude decay of strong motion records in northeastern United States and Canada.

Laboratory data suggest that in rocks where there is no fluid flow Q is constant over a wide range of frequency. Fluid motion in pores and cracks introduces a frequency dependent Q. Frequency dependence is strongly controlled by a critical frequency which is a function of crack or pore geometry, porosity, permeability and fluid viscosity. Below the critical frequency Q decreases with frequency and above the critical frequency, Q increases with frequency. This increase is proportional to the square root of frequency.

The increase of Q with frequency and proportionality constant ($Q \propto f^{0.5}$) is very close to values determined for the crust from the coda wave analysis. Since coda decay provides a measure of the intrinsic attenuation in the crust, it is reasonable to assume that, in addition to constant Q, fluid flow plays an important role in attenuation in the crust. For the Northeast, we find the intrinsic constant Q to be high ($500 \leq Q \leq 2000$). The fluid flow effects on attenuation are as large or larger than that of the intrinsic attenuation in the frequency range of 1 to 10 Hz.

The scattering analysis of strong motion records at 1 Hz and 5 Hz in the distance range of 10-200 km gives a large albedo ($B_0=0.9$), implying strong scattering. In addition to albedo the

13

only property of the scatterers that can be determined is the scattering extinction length. We obtain an extinction length of about 17 km for $f=1$ Hz and 5 Hz. The scatterers could be geologic fractures such as individual plutons, rock type changes, shear zones, dikes, sills or, most likely, a combination of all these.

It is important to state that the above discussions are based on a limited amount of data and theoretical models that make simplifying assumptions. It is necessary to analyze additional near-field data and to improve the models in order to draw firm conclusions.

Acknowledgements

15

REFERENCES

Aki, K., and Chouet, B., 1975, Origin of coda waves: source, attenuation and scattering effects, *J. Geophys. Res.*, 80, 3322-3342.

Aki, K., 1980, Attenuation of shear waves in the lithosphere for frequencies from 0.05 to 25 Hz, *Phys. Earth Planet. Inter.*, 21, 50-60.

Aki, K., and Richards, P.G., 1980, Quantitative seismology. Theory and methods. W.H. Freeman and Co., San Francisco.

Auriault, J.L., Borne, L., and Chambon, R., 1985, Dynamics of porous saturated media, checking of the generalized law of Darcy, *J. Acoust. Soc. Am.*, 77, 1641-1650.

Birch, F., and Bancroft, D., 1938, Elasticity and internal friction in a long column of granite, *Bull. Seism. Soc. Am.*, 28, 243-254.

Bradley, J.J., and Fort, A.N.Jr., 1966, Internal friction in rocks in *Handbook of Physical constants*, S.P. Clark, Jr., Ed. , GSA Publ., p. 175-193.

Brown, R.J.S., and Korringa, J., 1975, On the dependence of the elastic properties of a porous rock on the compressibility of the pore fluid, *Geophysics*, 40, 608-616.

Biot, M.A., 1956a, Theory of propagation of elastic waves in a fluid saturated porous solid. I. Low frequency range, *J. Acoust. Soc. Am.*, 28, 168-178.

Biot, M.A., 1956b, Theory of propagation of elastic waves in a fluid saturated porous solid. II. Higher frequency range, *J. Acoust. Soc. Am.*, 28, 179-191.

Biot, M.A., 1962, Mechanics of deformation and acoustic propagation in porous media, *J. Appl. Phys.*, 33, 1482-1488.

preceding page blank - not filmed

Clark, V.A., Spencer, T.W., Tittmann, B.R., Ahlberg, L.A., and Coombe, L.T., 1980, Effect of volatiles on attenuation Q^{-1} and velocity in sedimentary rocks, *J. Geophys. Res.*, 85, 5190-5198.

Dainty, A.M., Goins, N.R., and Toksöz, M.N., 1976, Seismic investigation of the lunar interior, *in* Lunar science VII: Houston Lunar Science Institute, p. 181-183.

Dainty, A.M., and Toksöz, M.N., 1977, Elastic wave propagation in a highly scattering medium. A diffusion approach, *J. Geophys.*, 43, 375-388.

Dainty, A.M., and Toksöz, M.N., 1981, Seismic codas on the Earth and the Moon: a comparison, *Phys. Earth and Plan. Int.*, 26, 250-260.

Dunn, K.J., 1985, Acoustic attenuation in fluid saturated porous cylinders at low frequencies, *J. Acoust. Soc. Am*, 79, 1709-1721.

Gao, L.S., Lee, L.C., Biswas, N.H., and Aki, K., 1983a. Comparison of the effects between single and multiple scattering on coda waves for local earthquakes, *Bull. Seism. Soc. Am.*, 73, 373-389.

Gao, L.S., Lee, L.C., Biswas, N.H., and Aki, K., 1983b. Effects of multiple scattering on coda waves in three-dimensional medium, *Pure and Apllied Geoph.*, 121, 3-15.

Gardner, GH.F., Wyllie, M.R.J., and Droschack, D.M., 1964, Effects of pressure and fluid saturation on the attenuation of elastic waves in sands, *J. Petr. Tech.*, 189-198.

Gupta, I.N., Burnetti, A., McElfresh, T.W., von Seggern, D.H., and Wagner, R.A., 1983, Lateral variations in attenuation of ground motion in the eastern United States based on propagation of L_g. NUREG/CR-3555, U.S. Nuclear Regulatory Commission, Washington, D.C.

Hermann, R.B., 1980, Q estimates using the coda of local earthquakes, *Bull. Seism. Soc. Am.*, 70,

447-468.

Johnston, D.H., and Toksöz, M.N., 1980, Ultrasonic P and S wave attenuation in dry and saturated rocks under pressure, *J. Geophys. Res.*, 85, 925-936.

Klima, K., Vanek, J., and Pros, Z., 1964, The attenuation of longitudinal waves in diabase and greywacke under pressure up to 4 kilobars, *Studia Geoph. et Geod.*, 8, 247-254.

Knopoff, L., 1964, Q, *Rev. Geophys.*, 2, 625-660.

Kopnichev, Y.F., 1977. The role of multiple scattering in the formation of a seismogram tail, *Izv. Acad. Sci., USSR, Phys. Solid Earth*, 13, 394-398.

Mason, W.P., Beshers, D.N., and kuo, J.T., 1970, Internal friction in Westerly granite: Relation to dislocation theory, *J. Appl. Phys.*, 41, 5206-5209.

Nur, A., and Winkler, K., 1980, The role of friction and fluid flow in wave attenuation in rocks (abst.), *Geophysics*, 45, 591-592.

O'Doherty, R.F., and Anstey, N.A., 1971. Reflections on amplitudes, *Geophys. Prospect.*, 19, 430-458.

Pandit, B.I., and Savage, J.C., 1973, An experimental test of Lomnitz's theory of internal friction in rocks, *J. Geophys. Res.*, 78, 6097-6099.

Peselnick, L., and Outerbridge, W.F., 1961, Internal friction in shear and shear modulus of Solenhofen limestone over a frequency range of 10^7 cycles per second, *J. Geophys. Res.*, 66, 581-588.

Plona, T.J., Observation of a second bulk compressional wave in a porous medium at ultrasonic frequencies, *Appl. Phys. Lett.*, 36, 256-261.

Plona, T.J., and Johnson, D.L., 1980, Experimental study of the two bulk compressional modes in

19

water saturated porous structures, *Ultrasonic Symposium*, 864-872.

Pulli, J., 1984, Attenuation of coda waves in New England, *Bull. Seism. Soc. Am.*, 74, 1149-1166.

Rautian, T.G., and Khalturin, V.I., 1978, The use of the coda for the determination of the earth-quake source spectrum, *Bull. Seism. Soc. Am.*, 63, 1809-1827.

Richards, P.G., and Menke, W., 1983. The apparent attenuation of a scattering medium, *Bull. Seism. Soc. Am.*, 73, 1005-1021.

Roecker, S.W., Tucker, B., King, J., and Hatzfled, D., 1982, Estimates of Q in central Asia as a function of frequency and depth using the coda of locally recorded earthquakes, *Bull. Seism. Soc. Am.*, 72, 129-149.

Schmitt, D.P., 1985, Simulation numérique de diagraphies acoustiques. Propagation d'ondes dans des formations cylindriques axisymétriques radialement stratifiées incluant des milieux élastiques et/ou poreux saturés. Ph.D. thesis. Grenoble Univ.

Singh, S., 1985, L_g and coda wave studies of Eastern Canada, Ph.D. thesis. Saint Louis University, Missouri.

Singh, S., and Hermann, R.B., 1983, Regionalization of crustal coda Q in the continental United States, *J. Geophys. Res.*, 88, 527-538.

Spencer, J.W., Jr., 1981, Stress relaxations at low frequencies in fluid saturated rocks: attenuation and modulus dispersion. *J. Geophys. Res.*, 86, 1803-1812.

Tittmann, B.R., Housley, R.M., Alers, G.A., and Cirlin, E.H., 1974, Internal friction in rocks and its relationship to volatiles on the moon, *in* Lunar Science Conf., 5th Proc., Geochim. et Cosmochim. Acta, suppl. 5, v.3, 2913-2918.

20

Tittmann, B.R., Nadler, H., Clark, V.A., Ahlberg, L.A., and Spencer, T.W., 1981, Frequency dependence of seismic dissipation in saturated rocks, *Geophys. Res. Lett.*, 8, 36-38.

Toksöz, M.N., Johnston, D.H., and Timur, A., 1979, Attenuation of seismic waves in dry and saturated rocks. I. Laboratory measurements, *Geophysics*, 44, 681-690.

Toksöz, M.N., and Johnston, D.H., 1981, Seismic wave attenuation. Editors. Geophysics reprint series No.2. Society of Exploration Geophysicist.

Walsh, J.B., 1966, Seismic wave attenuation in rock due to fracture, *J. Geophys. Res.*,17, 2591-2599.

Winkler , K., and Nur, A., 1979, Pore fluids and seismic attenuation in rocks, *Geophys. Res. Lett.*, 6, 1-4.

Wu, R.S., 1984. Multiple scattering and energy transfer of seismic waves and the application of the theory to Hindu Kush region, in "Seismic wave scattering and the small scall inhomogeneities in the lithosphere", Chapter 4, Ph.D. thesis, Mass. Inst. Tech., Cambridge, M.A.

Wu, R.S., 1985, Multiple scattering and energy transfer of seismic waves. Separation of scattering effect from intrinsic attenuation. I. Theoretical modelling., *Geophys. J. R. Astr. Soc.*, 82, 57-80.

Wu, R.S., and Aki, K., 1985, Multiple scattering and energy transfer of seismic waves. Separation of scattering effect from intrinsic attenuation. II. Application of the theory to Hindu Kush region. submitted to *J. Geophys. Res.* .

APPENDIX A

The elastic wave energy received by an isotropic point receiver in a random heterogeneous medium can be represented by the *average energy density* $E(\underline{r})$ at that point. The energy density in radiative transfer theory is defined as (see Wu, 1985):

$$E(\underline{r}) = \frac{1}{C} \int_{4\pi} I(\underline{r}, \hat{\Omega}) d\Omega \qquad (A-1)$$

where C is the wave velocity, and $I(\underline{r}, \hat{\Omega})$ is the *specific intensity or directional intensity*. It gives the power flowing within a unit solid angle in the direction $\hat{\Omega}$ ($\hat{\Omega}$ is the unit vector) received by a unit area perpendicular to $\hat{\Omega}$, in a unit frequency band. The specific intensity is defined for a frequency ω, which is omitted in the notation. Since the P wave energy is much smaller than the S wave energy for earthquakes, we consider here $I(\underline{r}, \hat{\Omega})$ as only the S wave energy by neglecting the mode converted energy from P waves. We assume here also that the wave energy described by $I(\underline{r}, \hat{\Omega})$ is depolarized, i.e. the energy is equally partitioned between the two orthogonal components of S waves. This agrees generally with the observations.

From the radiative transfer equations we can obtain the equation for the transfer energy density:

$$E(\underline{r}) = E_{in} e^{-\eta_e l} + \int_V \left[\eta_s E(\underline{r_1}) + \varepsilon(\underline{r_1}, \hat{\Omega}) \right] G_0(\underline{r} - \underline{r_1}) dV_1 \qquad (A-2)$$

where E_{in} is the incident field and,

$$\varepsilon(\underline{r_1}, \hat{\Omega}) = \frac{4\pi}{C} W(\underline{r_1}, \hat{\Omega}) \qquad (A-3)$$

is the source energy density function, where W is the source power spectral density, and

$$G_0(\underline{r_1} - \underline{r}) = \frac{e^{-\eta_e R}}{4\pi R^2} = \frac{e^{-\eta_e |r - r_1|}}{4\pi \, |\, r - r_1 \,|^2} \qquad (A-4)$$

22

In (A-2), suppose the incident field $E_{in} = 0$ and the isotropic point source is located at $\underline{r} = 0$, radiating total power P_0. Then,

$$\varepsilon(\underline{r}) = \frac{P_0}{C}\delta(\underline{r}) = E_0\delta(\underline{r}) \qquad (A-5)$$

and Equation (A-2) becomes:

$$E(\underline{r}) = E_0\frac{e^{-\eta_e r}}{4\pi r^2} + \int_V \eta_s E(\underline{r_1})\frac{e^{-\eta_e|\underline{r}-\underline{r_1}|}}{4\pi\,|\,\underline{r}-\underline{r_1}\,|^2}dV_1 \qquad (A-6)$$

Assuming $E_0 = 1$, the solution can be written as:

$$
\begin{aligned}
E(\underline{r}) &= \frac{\eta_e P_d}{4\pi r}\exp(-\eta_e d_0 r) + \frac{\eta_e}{4\pi r}\int_1^\infty f(s, B_0)\exp(-\eta_e r s)ds \\
&= E_d(r) + E_c(r)
\end{aligned}
\qquad (A-7)
$$

where

$$P_d = \frac{2d_0^2(1-d_0^2)}{B_0(d_0^2 + B_0 - 1)} \qquad (A-8)$$

and d_0 is the diffuse multiplier determined by:

$$\frac{B_0}{2d_0}\ln\left\{\frac{1+d_0}{1-d_0}\right\} = 1; \qquad (A-9)$$

and

$$f(s, B_0) = \left\{\left[1 - \frac{B_0}{s}\tanh^{-1}(\frac{1}{s})\right]^2 + \left(\frac{\pi}{2}\frac{B_0}{s}\right)^2\right\}^{-1} \qquad (A-10)$$

The first term in Equation (A-7) is the diffuse term E_d and the second term is the coherent term E_c.

Note that the diffuse multiplier d_0 is always less than 1. When distance r is large, especially for large B_0, the diffuse term becomes dominant, and $E(r)$ will be approximately an exponential decay with an apparent attenuation coefficient $d_0\eta_e$, which is less than the extinction coefficient η_e.

23

The degree of reduction depends on the albedo B_0. Figure 1 shows the energy density distribution with distances for different albedo values.

APPENDIX B

Expressions of the elastic coefficients

The elastic coefficients A and N are equivalent to Lamé's coefficients. $\tilde{R}$ is a measure of the fluid pressure needed to move a given fluid volume into the porous aggregate, the total volume being constant. T is related to the fluid and solid volume variations. These coefficients can be easily expressed as functions of the bulk moduli of the solid K_s, the skeleton K_b and the fluid K_f, the shear modulus of the skeleton μ_b and the porosity $\tilde{\phi}$. Following Plona and Johnson (1980), one has:

$$
\begin{cases}
A &= \dfrac{(1-\tilde{\phi})(1-\tilde{\phi}-\dfrac{K_b}{K_s})K_s + \tilde{\phi}\dfrac{K_s}{K_f}K_b}{1-\tilde{\phi}-\dfrac{K_b}{K_s}+\tilde{\phi}\dfrac{K_s}{K_f}} - \dfrac{2}{3}N \\[4ex]
T &= \dfrac{(1-\tilde{\phi}-\dfrac{K_b}{K_s})\tilde{\phi}K_s}{1-\tilde{\phi}-\dfrac{K_b}{K_s}+\tilde{\phi}\dfrac{K_s}{K_f}} \\[4ex]
\tilde{R} &= \dfrac{\tilde{\phi}^2 K_s}{1-\tilde{\phi}-\dfrac{K_b}{K_s}+\tilde{\phi}\dfrac{K_s}{K_f}} \\[4ex]
N &= \mu_b
\end{cases}
\tag{B-1}
$$

In the above expression, it is assumed that the porosity does not vary with the pore pressure (Brown and Korringa, 1975; Dunn, 1985).

Denoting α_m and β_m, the compressional and shear wave velocities of the dry rock, one can write:

$$
\begin{aligned}
K_b &= (1-\tilde{\phi})\rho_s(\alpha_m^2 - 4\beta_m^2/3) \\
N &= (1-\tilde{\phi})\rho_s\beta_m^2
\end{aligned}
\tag{B-2}
$$

and for the fluid

$$
K_f = \rho_f\alpha_m^2
\tag{B-3}
$$

25

If one assumes an anelastic attenuation for the P and S waves in the skeleton characterized by quality factors Q_{α_m} and Q_{β_m} and a frequency dependence $e^{i\omega t}$, it implies a velocity dispersion of the form, (e.g. Aki and Richards, 1980):

$$c(\omega) = \frac{c(\omega_0)}{\left(1 - \frac{1}{\pi Q}\text{Log}(\frac{\omega}{\omega_0})\right)\left(1 - \frac{i}{2Q}\right)} \qquad (B-4)$$

where

- ω_0 is a reference angular frequency

- $c(\omega)$ is the body wave velocity (α_m or β_m) at angular frequency ω,

- Q is the corresponding quality factor (Q_{α_m} or Q_{β_m}).

In these conditions, α_m and β_m become complex and frequency dependent as well as K_b and the coefficients A, N, T and $\tilde{R}$.

The parameters chosen for the formation are α_m=5500 m/s; β_m=3300 m/s, K_s= 4.5 10^{10} Pa, and ρ_s=2700 kgm^{-3}. When introduced, the quality factor is identical for both body waves of the skeleton and is equal to 500.

26

Figure Captions

Figure 1. Schematic illustration of earthquake strong ground motion attenuation mechanism discussed in this paper. a) Rock anelasticity refers to frequency independent Q associated with relative motions and frictional losses across grains and dislocations. b) Scattering is due to structural and geologic heterogeneities in the crust. c) Fluid flow incorporates fluid motions in pores and fractures induced by P and S waves.

Figure 2. Normalized energy distribution curves corrected for spherical spreading, $4\pi r^2 E(r)$ as a function of normalized distance $D_e = r/L_e$ where L_e is the extinction length defined by Equation 6 in the text.

Figures 3a,b. Ground velocity (PSV) at 5 Hz (3a) and 1 Hz (2a) as a function of distance for events in northeastern United States and Eastern Canada. Values normalized to a common magnitude. Data are from compilation of Risk Engineering, Inc., under EPRI sponsorship. The solid line in each case is a "best" fit to data.

$\triangle$ 11-1-82, New Brunswick, $M - b = 5.5$, ECTN data

$\bigcirc$ 19-1-82, New Hampshire, $M_b = 4.8$, strong motion data and ECTN

$\square$ 31-3-82, New Brunswick, $M_b = 4.8$, strong motion data and ECTN

$\diamondsuit$ 6-5-82, New Brunswick, $M_b = 4.0$, strong motion data

$\triangle$ 16-6-82, New Brunswick, $M_b = 4.6$, strong motion data and ECTN

$\bigcirc$ 7-10-83, Adirondacks, New York, $M_b = 5.6$, ECTN

$\square$ 11-10-83, Ottawa, Canada, $M_b = 4.1$, ECTN

Figure 4a,b. Match between the multiple scattering model ($B_o = 0.9$ and $L_e = 15$ km) and the observed ground motion data as a function of radial (epicentral) distance R, at frequencies 5 Hz (4a) and 1 Hz (4b). PSV curves are the "best" fit curves of Figures 3a,b. $(PSV \cdot R/10)$ and $(PSV \cdot R/10)^2$ are calculated from PSV curves. Note the goodness of fit between the model and data curves in the distance range of $R = 10$ to 100 km where model approximations are valid.

Figure 5. Sensitivity of theoretical curves (Power versus radial distance) at $f = 5$ Hz, to different model parameters. The model that fit the data best is shown as a "heavy" line.

Figure 6. Sensitivity of theoretical curves to albedo (B_o) values at $f = 5$ Hz as a function of distance. Fixed parameters are $L_e = 15$ km, $Q_a = 1350$. The model that fit the data best is shown as a solid line.

Figure 7. Velocity and attenuation (Q^{-1}) of P and S waves, as a function of frequency, due to fluid flow. The three models are for different porosity (ϕ) and permeability (k) values of fractured rock. A: $\phi = 0.5\%$, $k = 50$ darcies; B: $\phi = 1\%$, $k = 100$ darcies; C: $\phi = 2\%$, $k = 200$ darcies. The rock anelasticity is assumed to be zero. Note that velocity dispersion is small, but changes in attenuation are significant.

Figure 8. Velocity and attenuation of P and S waves due to fluid flow and rock anelasticity ($Q_0 = 500$). All other parameters are the same as those of Figure 7.
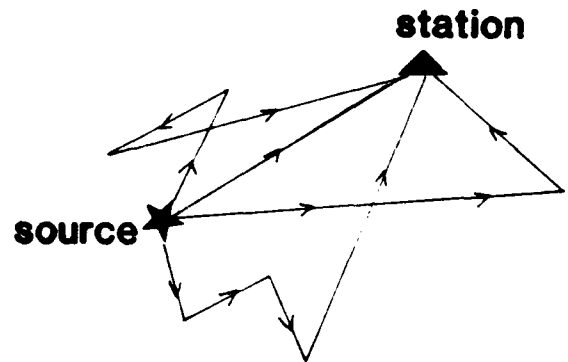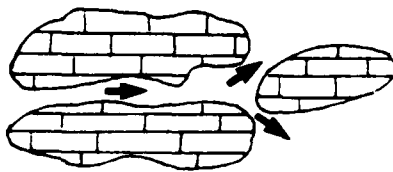
ATTENUATION MECHANISM
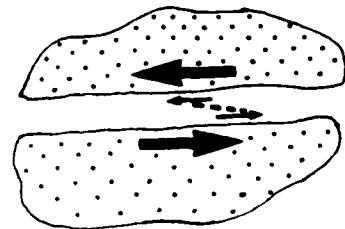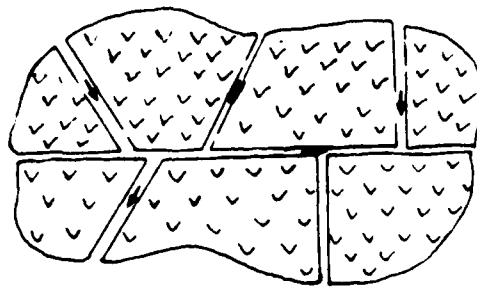
a – Rock Anelasticity
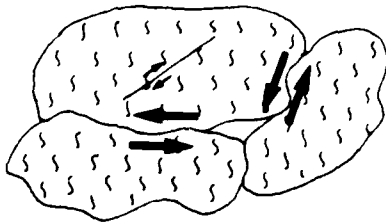
b – Multiple Scattering

c – Fluid Flow

Pressure driven flow

Shear driven flow

Fractures

Figure 1
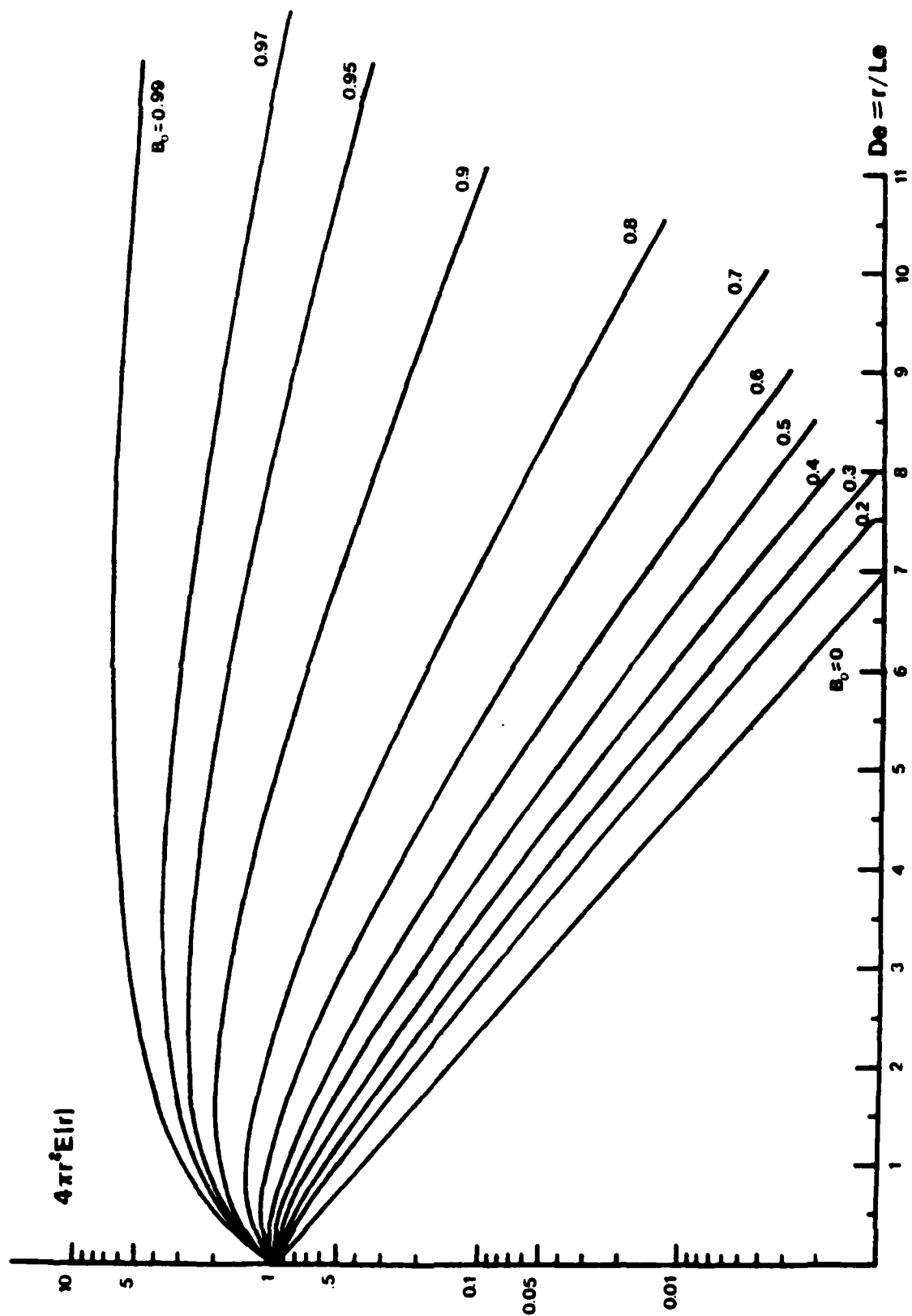
Figure 2
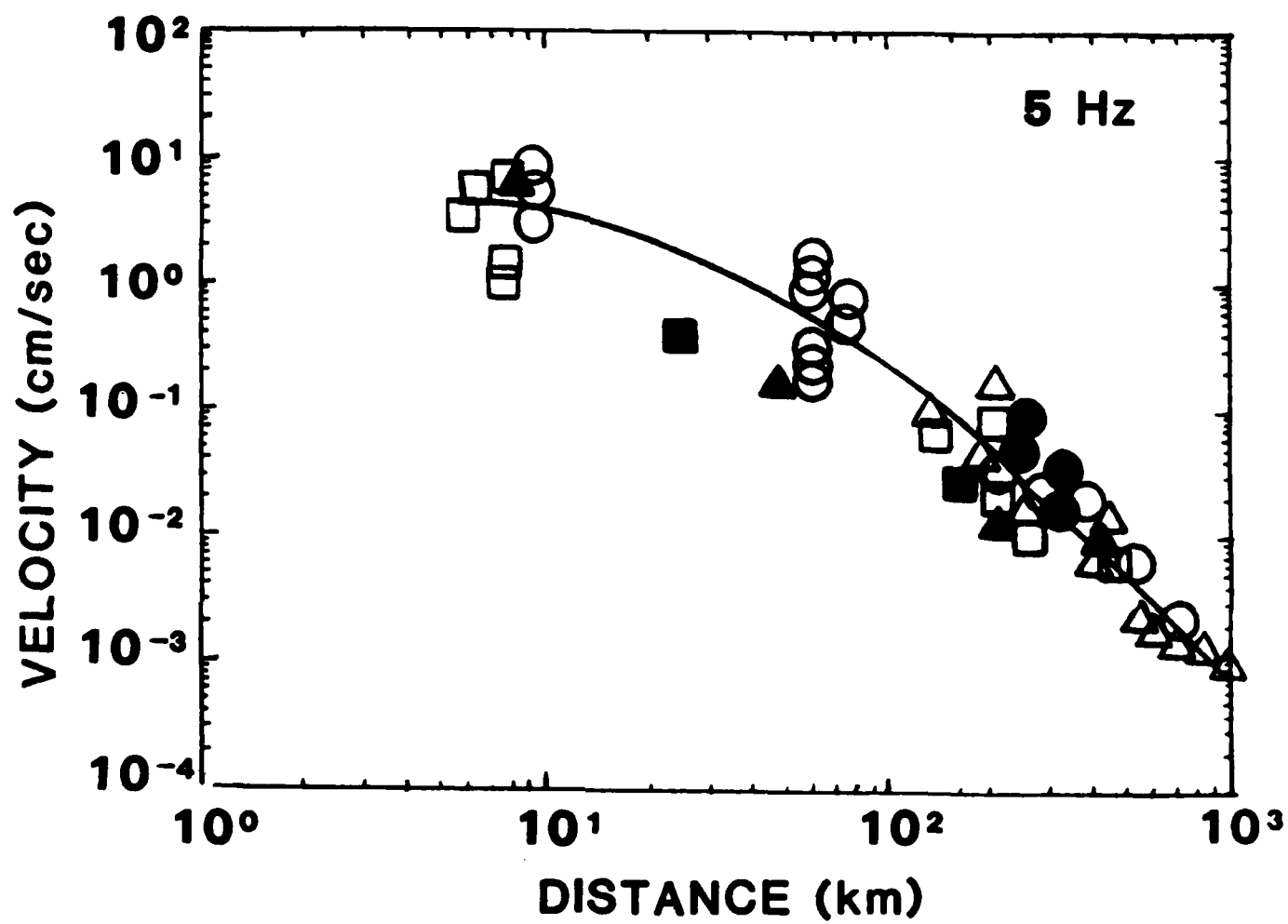
30

5 Hz

Figure 3a
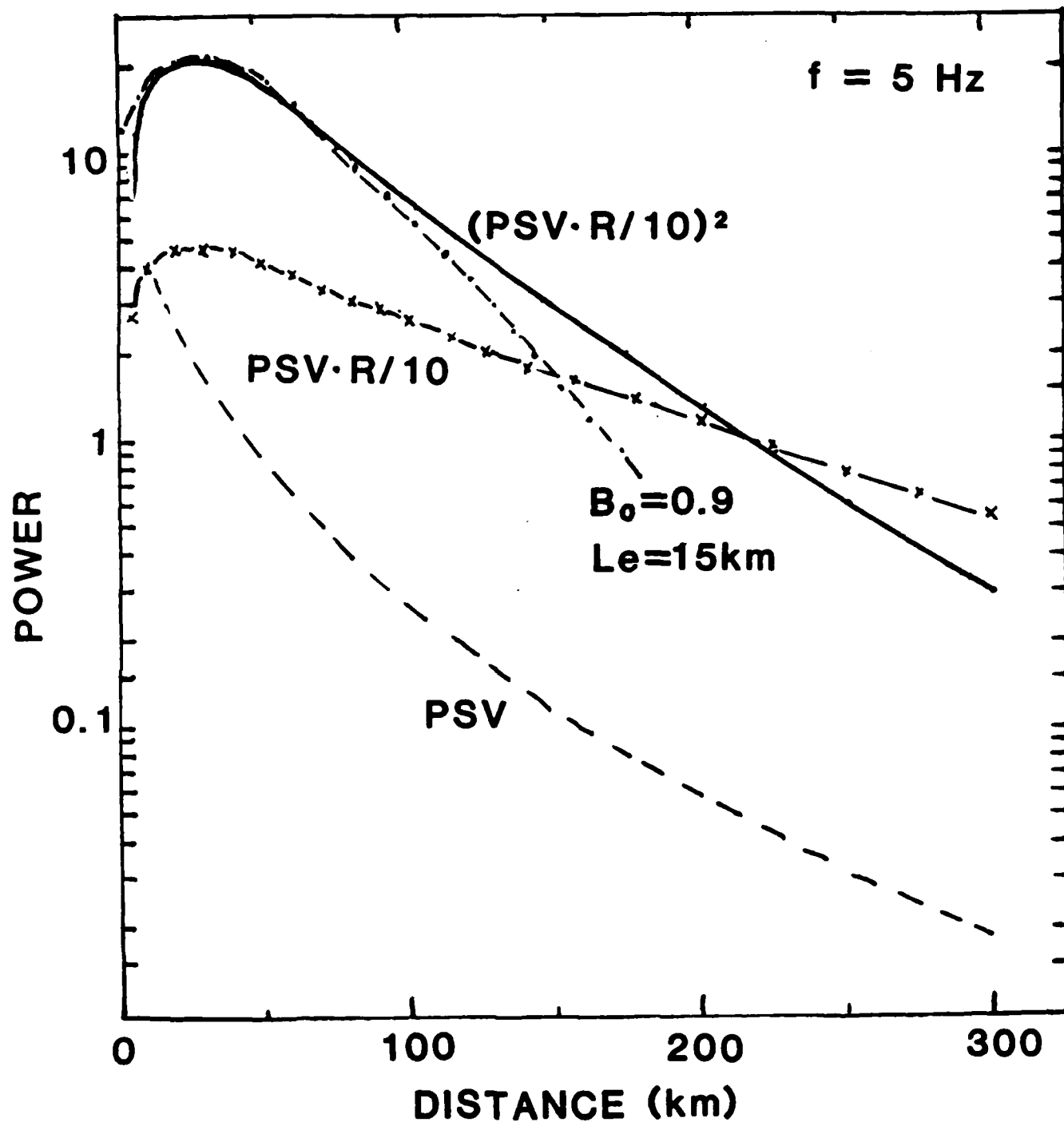
31

Figure 3b

32

f = 5 Hz

$(PSV \cdot R/10)^2$

$PSV \cdot R/10$

$B_0 = 0.9$
$Le = 15km$

PSV

POWER

DISTANCE (km)

Figure 4a

33

Figure 4b

34

f = 5 Hz

B_0=0.9, Le=20km

B_0=0.9, Qa=1350

B_0=0.8, Qa=675

B_0=0.7, Qa=450

Le=15km

B_0=0.5, Qa=270

B^0=0, Qa=135

POWER

DISTANCE (km)

Figure 5

35

POWER (y-axis) vs DISTANCE (km) (x-axis)

$B_0 = 0$

$B_0 = 0.5$

$B_0 = 0.7$
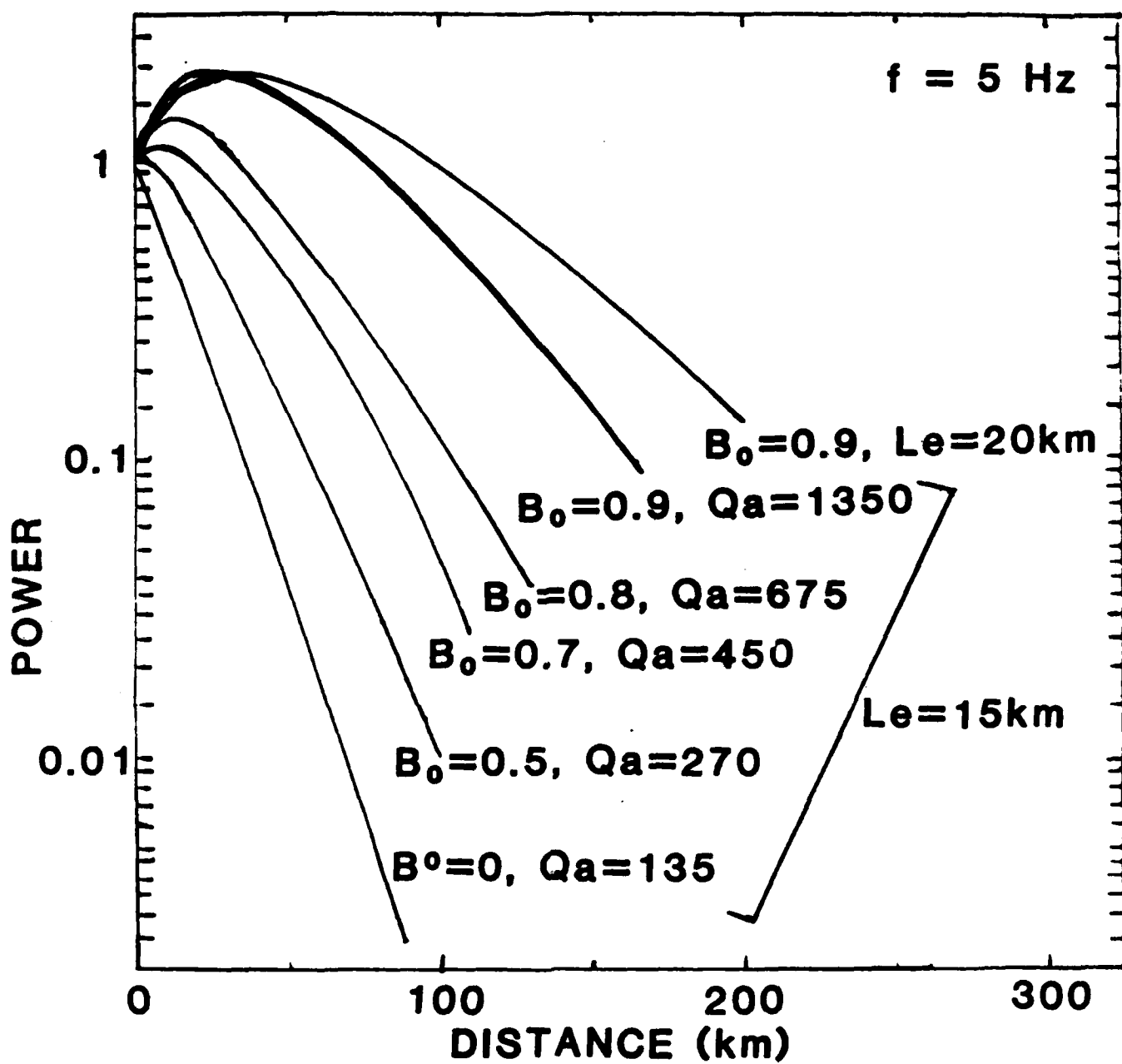
$B_0 = 0.8$

$B_0 = 0.9$
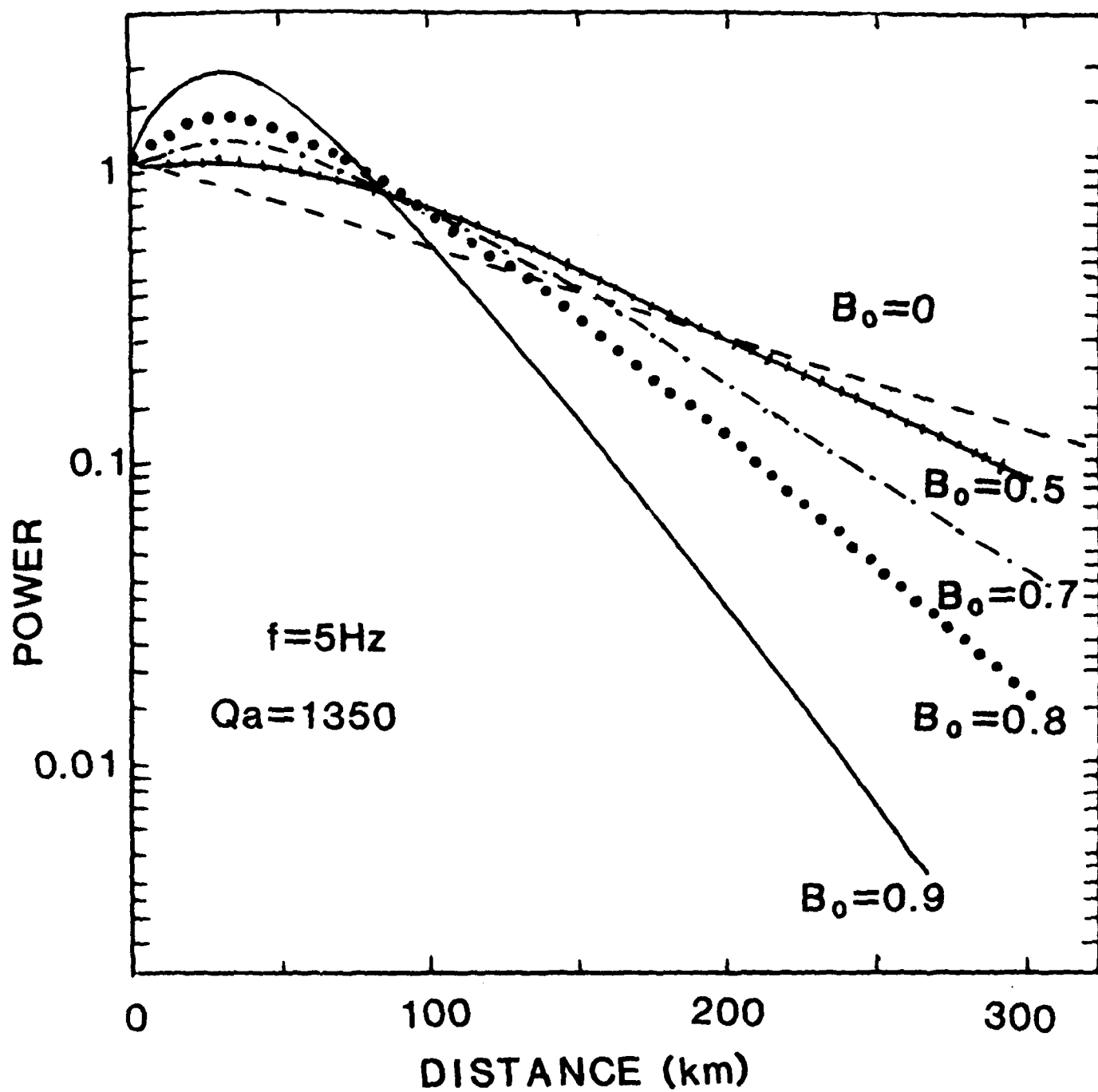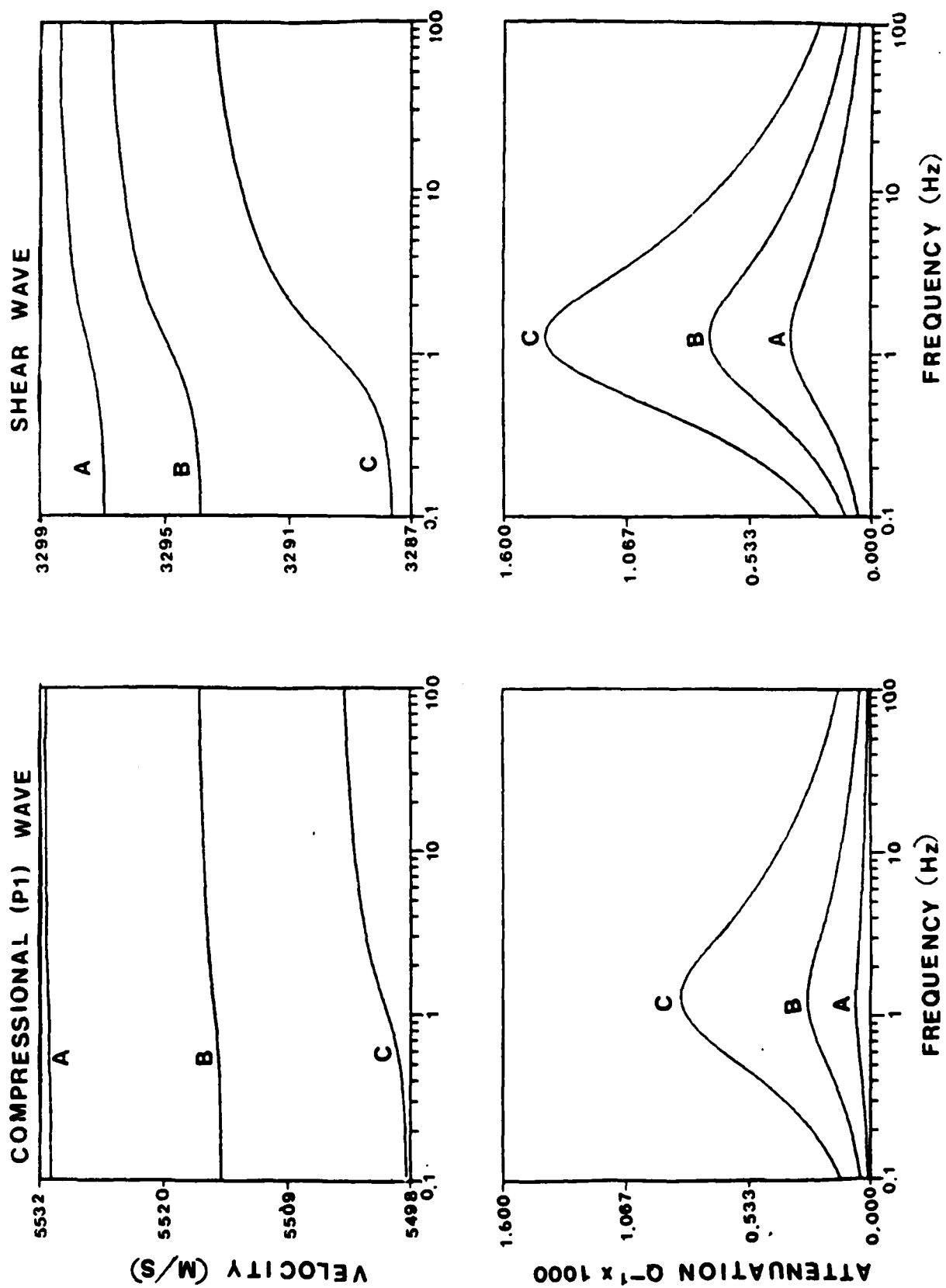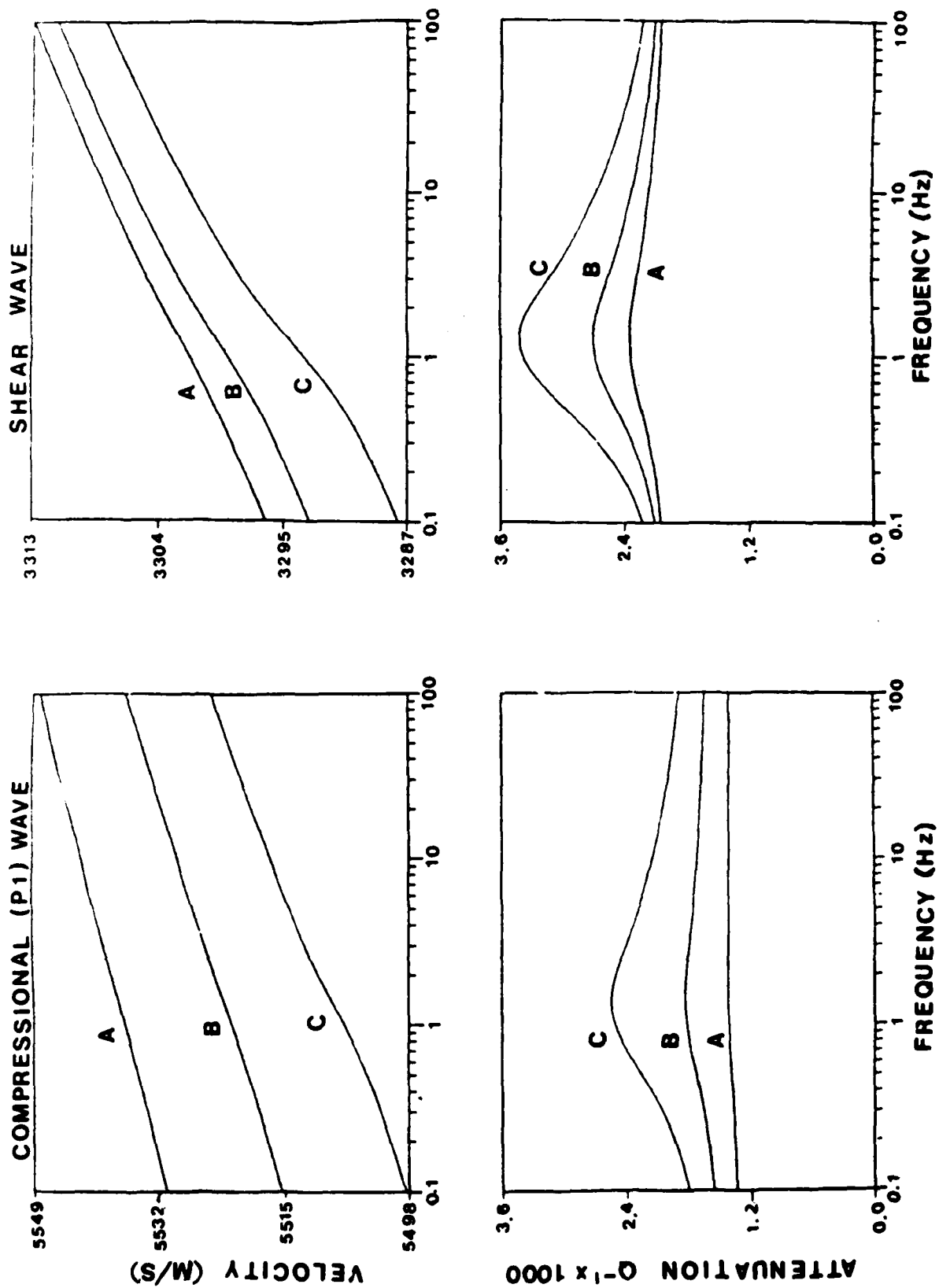
$f = 5Hz$

$Qa = 1350$

Figure 6

36

Figure 7

37

Figure 8

38
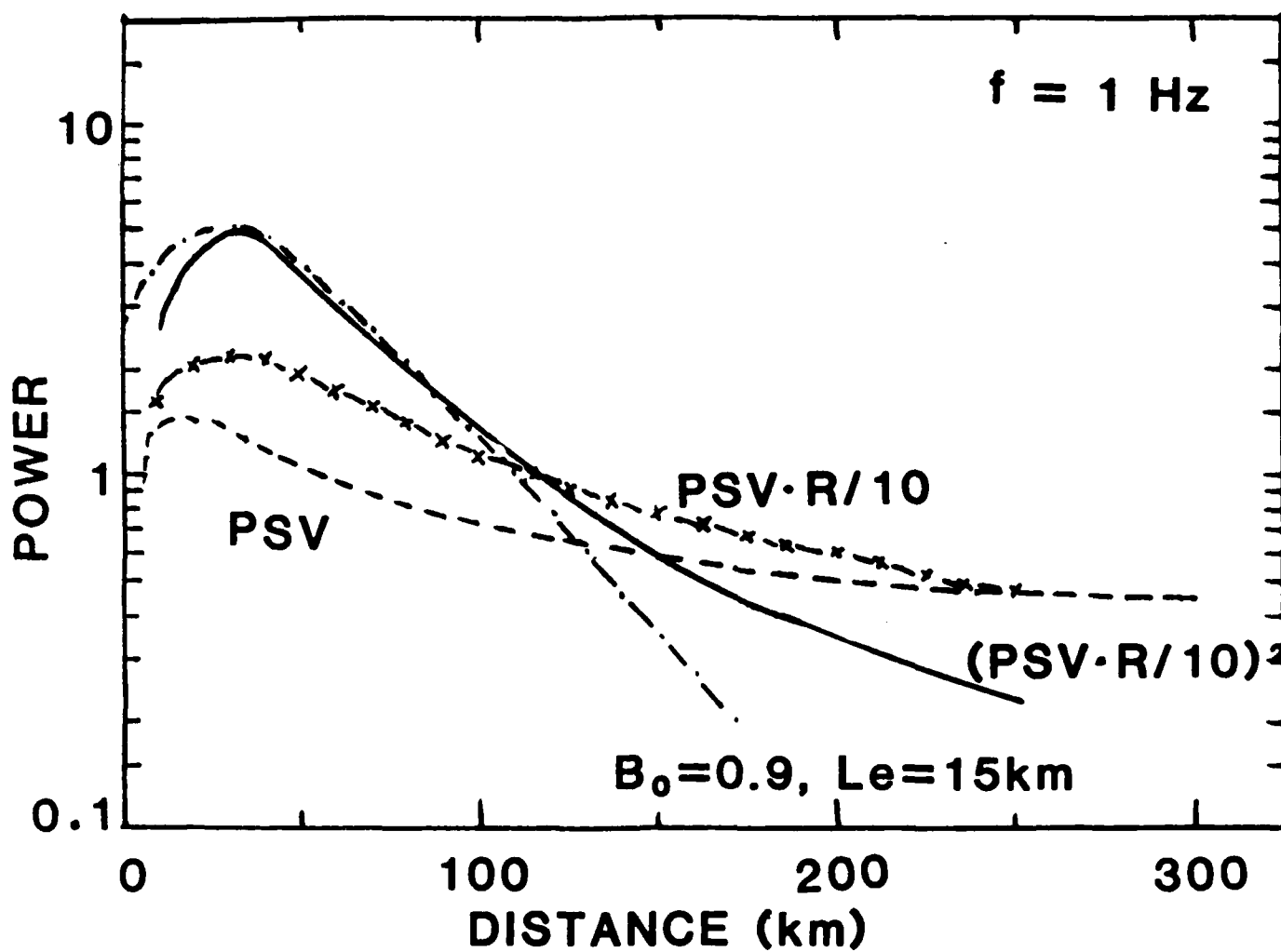
Professor Keiiti Aki
Center for Earth Sciences
University of Southern California
University Park
Los Angeles, CA 90089-0741

Professor Charles B. Archambeau
Cooperative Institute for Resch
  in Environmental Sciences
University of Colorado
Boulder, CO 80309

Dr. Thomas C. Bache Jr.
Science Applications Int'l Corp.
10210 Campus Point Drive
San Diego, CA 92121   (2 copies)

Dr. Douglas R. Baumgardt
Signal Analysis & Systems Div.
ENSCO, Inc.
5400 Port Royal Road
Springfield, VA 22151-2388

Dr. S. Bratt
Science Applications Int'l Corp.
10210 Campus Point Drive
San Diego, CA 92121

Dr. Lawrence J. Burdick
Woodward-Clyde Consultants
P.O. Box 93245
Pasadena, CA 91109-3245 (2 copies)

Professor Robert W. Clayton
Seismological Laboratory/Div. of
  Geological & Planetary Sciences
California Institute of Technology
Pasadena, CA 91125

Dr. Vernon F. Cormier
Department of Geology & Geophysics
U-45, Roon 207
The University of Connecticut
Storrs, Connecticut 06268

Dr. Zoltan A. Der
ENSCO, Inc.
5400 Port Royal Road
Springfield, VA 22151-2388

Professor John Ferguson
Center for Lithospheric Studies
The University of Texas at Dallas
P.O. Box 830688
Richardson, TX 75083-0688

Professor Stanley Flatte'
Applied Sciences Building
University of California, Santa Cruz
Santa Cruz, CA 95064

Professor Steven Grand
Department of Geology
245 Natural History Building
1301 West Green Street
Urbana, IL 61801

Professor Roy Greenfield
Geosciences Department
403 Deike Building
The Pennsylvania State University
University Park, PA 16802

Professor David G. Harkrider
Seismological Laboratory
Div of Geological & Planetary Sciences
California Institute of Technology
Pasadena, CA 91125

Professor Donald V. Helmberger
Seismological Laboratory
Div of Geological & Planetary Sciences
California Institute of Technology
Pasadena, CA 91125

Professor Eugene Herrin
Institute for the Study of Earth
 & Man/Geophysical Laboratory
Southern Methodist University
Dallas, TX 75275

Professor Robert B. Herrmann
Department of Earth & Atmospheric
        Sciences
Saint Louis University
Saint Louis, MO 63156

Professor Lane R. Johnson
Seismographic Station
University of California
Berkeley, CA 94720

Professor Thomas H. Jordan
Department of Earth, Atmospheric
 and Planetary Sciences
Mass Institute of Technology
Cambridge, MA 02139

Dr. Alan Kafka
Department of Geology &
  Geophysics
Boston College
Chestnut Hill, MA 02167

Professor Leon Knopoff
University of California
Institute of Geophysics
 & Planetary Physics
Los Angeles, CA 90024

Professor Charles A. Langston
Geosciences Department
403 Deike Building
The Pennsylvania State University
University Park, PA 16802

Professor Thorne Lay
Department of Geological Sciences
1006 C.C. Little Building
University of Michigan
Ann Harbor, MI 48109-1063

Dr. Randolph Martin III
New England Research, Inc.
P.O. Box 857
Norwich, VT 05055

Dr. Gary McCartor
Mission Research Corp.
735 State Street
P.O. Drawer 719
Santa Barbara, CA 93102   (2 copies)

Professor Thomas V. McEvilly
Seismographic Station
University of California
Berkeley, CA 94720

Dr. Keith L. McLaughlin
Teledyne Geotech
314 Montgomery Street
Alexandria, VA 22314

Professor William Menke
Lamont-Doherty Geological Observatory
 of Columbia University
Palisades, NY 10964

Professor Brian J. Mitchell
Department of Earth & Atmospheric
      Sciences
Saint Louis University
Saint Louis, MO 63156

Mr. Jack Murphy
S-CUBED
A Division of Maxwell Laboratory
11800 Sunrise Valley Drive
Suite 1212
Reston, VA 22091 (2 copies)

Professor Otto W. Nuttli
Department of Earth &
 Atmospheric Sciences
Saint Louis University
Saint Louis, MO 63156

Professor J. A. Orcutt
Institute of Geophysics and Planetary
  Physics, A-205
Scripps Institute of Oceanography
Univ. of California, San Diego
La Jolla, CA 92093

Professor Keith Priestley
University of Nevada
Mackay School of Mines
Reno, Nevada 89557

Professor Charles G. Sammis
Center for Earth Sciences
University of Southern California
University Park
Los Angeles, CA 90089-0741

Dr. Jeffrey L. Stevens
S-CUBED,
A Division of Maxwell Laboratory
P.O. Box 1620
La Jolla, CA 92038-1620

Professor Brian Stump
Institute for the Study of Earth & Man
Geophysical Laboratory
Southern Methodist University
Dallas, TX 75275

Professor Ta-liang Teng
Center for Earth Sciences
University of Southern California
University Park
Los Angeles, CA 90089-0741

Professor M. Nafi Toksoz
Earth Resources Lab
Dept of Earth, Atmospheric and
    Planetary Sciences
Massachusetts Institute of Technology
42 Carleton Street
Cambridge, MA 02142

Professor Terry C. Wallace
Department of Geosciences
Building #11
University of Arizona
Tucson, AZ 85721

Professor Francis T. Wu
Department of Geological Sciences
State University of new York
  At Binghamton
Vestal, NY 13901

Dr. Monem Abdel-Gawad
Rockwell Internat'l Science Center
1049 Camino Dos Rios
Thousand Oaks, CA 91360

Professor Shelton S. Alexander
Geosciences Department
403 Deike Building
The Pennsylvania State University
University Park, PA 16802

Dr. Muawia Barazangi
Geological Sciences
Cornell University
Ithaca, NY 14853

Mr. William J. Best
907 Westwood Drive
Vienna, VA 22180

Dr. N. Biswas
Geophysical Institute
University of Alaska
Fairbanks, AK 99701

Dr. G. A. Bollinger
Department of Geological Sciences
Virginia Polytechnical Institute
21044 Derring Hall
Blacksburg, VA 24061

Dr. James Bulau
Rockwell Int'l Science Center
1049 Camino Dos Rios
P.O. Box 1085
Thousand Oaks, CA 91360

Mr. Roy Burger
1221 Serry Rd.
Schenectady, NY 12309

Dr. Robert Burridge
Schlumberger-Doll Resch Ctr.
Old Quarry Road
Ridgefield, CT 06877

Science Horizons, Inc.
ATTN: Dr. Theodore Cherry
710 Encinitas Blvd., Suite 101
Encinitas, CA 92024 (2 copies)

Professor Jon F. Claerbout
Professor Amos Nur
Dept. of Geophysics
Stanford University
Stanford, CA 94305 (2 copies)

Dr. Anton W. Dainty
AFGL/LWH
Hanscom AFB, MA 01731

Professor Adam Dziewonski
Hoffman Laboratory
Harvard University
20 Oxford St.
Cambridge, MA 02138

Professor John Ebel
Dept of Geology & Geophysics
Boston College
Chestnut Hill, MA 02167

Dr. Alexander Florence
SRI International
333 Ravenwood Avenue
Menlo Park, CA 94025-3493

Dr. Donald Forsyth
Dept. of Geological Sciences
Brown University
Providence, RI 02912

Dr. Anthony Gangi
Texas A&M University
Department of Geophysics
College Station, TX 77843

Dr. Freeman Gilbert
Institute of Geophysics &
  Planetary Physics
Univ. of California, San Diego
P.O. Box 109
La Jolla, CA 92037

Mr. Edward Giller
Pacific Seirra Research Corp.
1401 Wilson Boulevard
Arlington, VA 22209

Dr. Jeffrey W. Given
Sierra Geophysics
11255 Kirkland Way
Kirkland, WA 98033

Dr. Arthur Lerner-Lam
Lamont-Doherty Geological Observatory
 of Columbia University
Palisades, NY 10964

Dr. L. Timothy Long
School of Geophysical Sciences
Georgia Institute of Technology
Atlanta, GA 30332

Dr. George R. Mellman
Sierra Geophysics
11255 Kirkland Way
Kirkland, WA 98033

Dr. Bernard Minster
Institute of Geophysics and Planetary
  Physics, A-205
Scripps Institute of Oceanography
Univ. of California, San Diego
La Jolla, CA 92093

Dr. Geza Nagy
SRI International
333 Ravenswood Avenue
Menlo Park, CA 94025-3493

Dr. Jack Oliver
Department of Geology
Cornell University
Ithaca, NY 14850

Dr. Robert Phinney/Dr. F.A. Dahlen
Dept of Geological
  Geophysical Sci. University
Princeton University
Princeton, NJ 08540 (2 copies)

Professor Paul G. Richards
Lamont-Doherty Geological
 Observatory of Columbia Univ.
Palisades, NY 10964

Dr. Norton Rimer
S-CUBED
A Division of Maxwell Laboratory
P.O. 1620
La Jolla, CA 92038-1620

Professor Larry J. Ruff
Department of Geological Sciences
1006 C.C. Little Building
University of Michigan
Ann Arbor, MI 48109-1063

Dr. Alan S. Ryall, Jr.
Center of Seismic Studies
1300 North 17th Street
Suite 1450
Arlington, VA 22209-2308   (4 copies)

Dr. David G. Simpson
Lamont-Doherty Geological Observ.
  of Columbia University
Palisades, NY 10964

Dr. Bob Smith
Department of Geophysics
University of Utah
1400 East 2nd South
Salt Lake City, UT 84112

Dr. S. W. Smith
Geophysics Program
University of Washington
Seattle, WA 98195

Rondout Associates
ATTN: Dr. George Sutton,
Dr. Jerry Carter, Dr. Paul Pomeroy
P.O. Box 224
Stone Ridge, NY 12484 (4 copies)

Dr. L. Sykes
Lamont Doherty Geological Observ.
Columbia University
Palisades, NY 10964

Dr. Pradeep Talwani
Department of Geological Sciences
University of South Carolina
Columbia, SC 29208

Dr. R. B. Tittmann
Rockwell International Science Center
1049 Camino Dos Rios
P.O. Box 1085
Thousand Oaks, CA 91360

Weidlinger Associates
ATTN: Dr. Gregory Wojcik
620 Hansen Way, Suite 100
Palo Alto, CA 94304

Professor John H. Woodhouse
Hoffman Laboratory
Harvard University
20 Oxford St.
Cambridge, MA 02138

Dr. Gregory B. Young
ENSCO, Inc.
5400 Port Royal Road
Springfield, VA 22151-2388

Dr. Peter Basham
Earth Physics Branch
Geological Survey of Canada
1 Observatory Crescent
Ottawa, Ontario
CANADA K1A 0Y3

Dr. Eduard Berg
Institute of Geophysics
University of Hawaii
Honolulu, HI 96822

Dr. Michel Bouchon - Universite
   Scientifique et Medicale de Grenob
Lab de Geophysique - Interne et
   Tectonophysique - I.R.I.G.M-B.P.
38402 St. Martin D'Heres
Cedex FRANCE

Dr. Hilmar Bungum/NTNF/NORSAR
P.O. Box 51
Norwegian Council of Science,
Industry and Research, NORSAR
N-2007 Kjeller, NORWAY

Dr. Michel Campillo
I.R.I.G.M.-B.P. 68
38402 St. Martin D'Heres
Cedex, FRANCE

Dr. Kin-Yip Chun
Geophysics Division
Physics Department
University of Toronto
Ontario, CANADA M5S 1A7

Dr. Alan Douglas
Ministry of Defense
Blacknest, Brimpton,
 Reading RG7-4RS
UNITED KINGDOM

Dr. Manfred Henger
Fed. Inst. For Geosciences & Nat'l Res.
Postfach 510153
D-3000 Hannover 51
FEDERAL REPUBLIC OF GERMANY

Dr. E. Husebye
NTNF/NORSAR
P.O. Box 51
N-2007 Kjeller, NORWAY

Tormod Kvaerna
NTNF/NORSAR
P.O. Box 51
N-2007 Kjeller, NORWAY

Mr. Peter Marshall, Procurement
 Executive, Ministry of Defense
Blacknest, Brimpton,
 Reading FG7-4RS
UNITED KINGDOM (3 copies)

Dr. Ben Menaheim
Weizman Institute of Science
Rehovot, ISRAEL 951729

Dr. Svein Mykkeltveit
NTNF/NORSAR
P.O. Box 51
N-2007 Kjeller, NORWAY (3 copies)

Dr. Robert North
Geophysics Division
Geological Survey of Canada
1 Observatory crescent
Ottawa, Ontario
CANADA, K1A OY3

Dr. Frode Ringdal
NTNF/NORSAR
P.O. Box 51
N-2007 Kjeller, NORWAY

Dr. Jorg Schlittenhardt
Federal Inst. for Geosciences & Nat'l Res.
Postfach 510153
D-3000 Hannover 51
FEDERAL REPUBLIC OF GERMANY

University of Hawaii
Institute of Geophysics
ATTN: Dr. Daniel Walker
Honolulu, HI 96822

Dr. Ramon Cabre, S.J.
c/o Mr. Ralph Buck
Economic Consular
American Embassy
APO Miami, Florida 34032

Professor Peter Harjes
Institute for Geophysik
Rhur University/Bochum
P.O. Box 102148, 4630 Bochum 1
FEDERAL REPUBLIC OF GERMANY

Professor Brian L.N. Kennett
Research School of Earth Sciences
Institute of Advanced Studies
G.P.O. Box 4
Canberra 2601
AUSTRALIA

Dr. B. Massinon
Societe Radiomana
27, Rue Claude Bernard
7,005, Paris, FRANCE (2 copies)

Dr. Pierre Mechler
Societe Radiomana
27, Rue Claude Bernard
75005, Paris, FRANCE

Dr. Ralph Alewine III
DARPA/NMRO
1400 Wilson Boulevard
Arlington, VA 22209-2308

Dr. Peter Basham
Geological Survey of Canada
1 Observatory Creseut
Ottowa, Ontario
CANADA K1A OY3

Dr. Robert Blandford
DARPA/NMRO
1400 Wilson Boulevard
Arlington, VA 22209-2308

Sandia National Laboratory
ATTN: Jr. H. B. Durham
Albuquerque, NM 87185

Dr. Jack Evernden
USGS-Earthquake Studies
345 Middlefield Road
Menlo Park, CA 94025

U.S. Geological Survey
ATTN: Dr. T. Hanks
Nat'l Earthquake Resch Center
345 Middlefield Road
Menlo Park, CA 94025

Dr. James Hannon
Lawrence Livermore Nat'l Lab.
P.O. Box 808
Livermore, CA 94550

U.S. Arms Control & Disarm. Agency
ATTN: Mrs. M. Hoinkes
Div. of Multilateral Affairs
Room 5499
Washington, D.C. 20451

Paul Johnson
ESS-4, Mail Stop J979
Los Alamos National Laboratory
Los Alamos, NM 87545

Ms. Ann Kerr
DARPA/NMRO
1400 Wilson Boulevard
Arlington, VA 22209-2308

Dr. Max Koontz
US Dept of Energy/DP 331
Forrestal Building
1000 Independence Ave.
Washington, D.C. 20585

Dr. W. H. K. Lee
USGS
Office of Earthquakes, Volcanoes,
  & Engineering
Branch of Seismology
345 Middlefield Rd
Menlo Park, CA 94025

Dr. William Leith
USGS
Mail Stop 928
Reston, VA 22092

Dr. Robert Masse'
Box 25046, Mail Stop 967
Denver Federal Center
Denver, Colorado 80225

Dr. Keith K. Nakanishi
Lawrence Livermore National Laboratory
P.O. Box 808, L-205
Livermore, CA 94550 (2 copies)

Dr. Carl Newton
Los Alamos National Lab.
P.O. Box 1663
Mail Stop C335, Group E553
Los Alamos, NM 87545

Dr. Kenneth H. Olsen
Los Alamos Scientific Lab.
Post Office Box 1663
Los Alamos, NM 87545

Howard J. Patton
Lawrence Livermore National Laboratory
P.O. Box 808, L-205
Livermore, CA 94550

HQ AFTAC/TG
Attn: Dr. Frank F. Pilotte
Patrick AFB, Florida 32925-6001

Mr. Jack Rachlin
USGS - Geology, Rm 3 C136
Mail Stop 928 National Center
Reston, VA 22092

Robert Reinke
AFWL/NTESG
Kirtland AFB, NM 87117-6008

HQ AFTAC/TGR
Attn: Dr. George H. Rothe
Patrick AFB, Florida 32925-6001

Donald L. Springer
Lawrence Livermore National Laboratory
P.O. Box 808, L-205
Livermore, CA 94550

Dr. Lawrence Turnbull
OSWR/NED
Central Intelligence Agency
CIA, Room 5G48
Washington, D.C. 20505

Dr. Thomas Weaver
Los Alamos Scientific Laboratory
Los Almos, NM 97544

AFGL/SULL
Research Library
Hanscom AFB, MA 01731-5000 (2 copies)

Secretary of the Air Force (SAFRD)
Washington, DC 20330
Office of the Secretary Defense
DDR & E
Washington, DC 20330

HQ DNA
ATTN: Technical Library
Washington, DC 20305

Director, Technical Information
DARPA
1400 Wilson Blvd.
Arlington, VA 22209

AFGL/XO
Hanscom AFB, MA 01731-5000

AFGL/LW
Hanscom AFB, MA 01731-5000

DARPA/PM
1400 Wilson Boulevard
Arlington, VA 22209

Defense Technical
 Information Center
Cameron Station
Alexandria, VA 22314
(12 copies)

Defense Intelligence Agency
Directorate for Scientific &
 Technical Intelligence
Washington, D.C. 20301

Defense Nuclear Agency/SPSS
ATTN: Dr. Michael Shore
6801 Telegraph Road
Alexandria, VA 22310

AFOSR/NPG
ATTN: Major John Prince
Bldg 410, Room C222
Bolling AFB, Wash D.C. 20332

AFTAC/CA (STINFO)
Patrick AFB, FL 32925-6001